A Very Large Lepton Collider in the VLHC tunnel

Tanaji Sen
FNAL, P.O. Box 500, Batavia, IL 60510
and
Jim Norem
ANL, Argonne, IL

February 8, 2001

Contents

`Issues still to be addressed`

- `Energy sawtooth, distributed RF`
- `Realistic estimates of TMCI thresholds`
- `Multi-bunch instabilities`
- `Beam-beam footprints (long-range if 1 ring, head-on if 2 rings)`
- `Use as a SR source`

1 Introduction

Plans for the future very large hadron collider (VLHC) now envisage a staging scenario [1] where a low field collider would be built first followed by a high field collider in the same tunnel several years later. There is also interest in an electron-positron collider in the same tunnel which could study physics that would complement the studies with the hadron collider e.g. (`fill in physics issues`....). The very large circumference of the tunnel makes it possible to think of an $e^+ - e^-$ ring which could reach an energy about twice that of LEP if we limit the synchrotron radiation power to 100MW. Compared to the NLC, the energy and luminosity reach of such a machine is lower. However the technology required is proven and available today. We believe that such a large lepton collider can be built with conservative assumptions and at a fraction of the current estimated cost of the NLC. In this paper we outline the design of this collider and consider some of the accelerator physics issues. We compare and contrast the parameters of this machine with LEP. Much of the material on LEP is gleaned from a recent paper by Brandt et al. [2].

2 Design Strategy

Our design philosophy of this electron-positron collider will be to to avail of the maximum RF power available and operate at the beam-beam limit The synchrotron radiation power lost by *both beams*, each with beam current I is

$$P_T = 2C_\gamma \frac{E^4 I}{e\rho} \ , \quad C_\gamma = \frac{4\pi}{3}\frac{r_e}{(m_e c^2)^3} = 8.86 \times 10^{-5} \ [\mathrm{m/GeV^3}] \tag{2.1}$$

Assuming that there are M_b bunches in each beam with bunch intensities N_b, the luminosity is

$$\mathcal{L} = \frac{f_{rev}}{4\pi}\frac{M_b N_b^2}{\sigma_x^* \sigma_y^*} \tag{2.2}$$

We will assume flat beams so that $\sigma_y^* \ll \sigma_x^*$. With this assumption, the vertical beam-beam tune shift is

$$\xi_y = \frac{r_e}{2\pi}\frac{N_b\beta_y^*}{\gamma\sigma_x^*\sigma_y^*} \tag{2.3}$$

Eliminating one power of N_b from the expression for the luminosity, we can write

$$\mathcal{L} = \frac{1}{2er_e}\frac{\xi_y}{\beta_y^*}\gamma I \tag{2.4}$$

I is the beam current in a single beam. Our strategy as stated earlier is that as we change parameters, P_T and ξ_y will be held constant.

Using Equation (2.4) to eliminate the current, we obtain the following equation for the luminosity and energy in terms of the fixed parameters and the bending radius ρ,

$$\boxed{\mathcal{L}\gamma^3 = \frac{3}{16\pi r_e^2(m_e c^2)}\frac{\xi_y P_T}{\beta_y^*}\rho} \tag{2.5}$$

We interpret this equation to imply that when the luminosity, synchrotron radiation power and beam-beam parameter are held fixed, the maximum energy of the ring increases with the third root of the machine circumference, i.e.

$$E \propto \rho^{1/3}$$

We should note that this determines the maximum allowable energy at these parameters. We can choose to operate at a lower energy to stay below the limits on either the radiation power or the beam-beam parameter. In the above equation β_y^* may be assumed constant only if the IR quadrupoles do not pose an aperture limitation in the vertical plane at any energy. We will assume that to be the case.

2.1 Bunch intensity limitations

The dominant limitation on the bunch intensity at collision energy arises due to the beam-beam interactions. We have incorporated this constraint in our scaling of the luminosity with energy, Equation (2.5). Another limitation that is more severe at injection energy is the Transverse Mode Coupling Instability (TMCI). As in the classical head-tail instability, synchrotron motion which exchanges particles in the head and tail of the bunch drives the instability but this instability can arise even with zero chromaticity. In the presence of transverse impedances (typically wall resistivity), the wake forces excited by particles in the head can exert strong enough forces on the tail such that betatron modes $\omega_\beta + m\omega_s$ are modified. Typically, at the threshold intensity of the instability, the modes $m = 0$ and $m = -1$ become degenerate. TMCI is known to limit the bunch current in LEP to below 1mA [2].

The threshold bunch current is given by

$$I_b^{TMCI} \simeq \frac{8 f_{rev}\nu_s E}{e\sum_i \beta_i k_{\perp\, i}(\sigma_s)} \tag{2.6}$$

where ν_s is the synchrotron frequency, the sum in the denominator is over tranverse impedances and $k_{\perp\, i}$ is a bunch length dependent transverse mode loss factor. Obviously higher synchrotron frequencies and longer bunches increase the threshold intensity. At LEP larger RF voltages are used to increase ν_s while emittance wigglers are used to increase the bunch length at the injection energy of 20GeV. Compared to LEP, the very large lepton collider has a revolution frequency that is an order of magnitude smaller while the synchrotron frequency, injection energy and bunch length are comparable. Various schemes have been proposed to combat TMCI for the low-field hadron collider [4], e.g. starting with lower intensity bunches at injection energy and coalescing at higher energy, feedback systems etc. We will assume that some such compensation scheme will be available for the lepton collider if necessary and that bunch currents of the order of 0.1mA will be acceptable.

`Realistic estimates of the likely transverse impedance would be helpful here.`

2.2 Beam intensity limitations

The available RF power determines the beam current to zeroth order. This constraint will be used in the design strategy in this report. However there are other sources of limitations which need to be considered as the design evolves. Perhaps the most important of these secondary limitations is the available cryogenic cooling power. We will assume that superconducting cavities will be used. The dynamic heat load on these cavities includes contributions from the RF dissipation and the beam induced heat load from both beams. These two sources lead to a power dissipation given by

$$P_{dynamic} = N_{cav}\frac{V_{RF}^2}{(R/Q)Q} + 2R_m(\sigma_s)I_bI_e \tag{2.7}$$

where N_{cav} is the number of cavities, (R/Q) is the normalized shunt impedance per cavity, Q is the unloaded quality factor of the cavities which depends on the operating temperature and the field gradient, R_m is a bunch length dependent loss impedance of the cavities, I_b is the bunch current, I_e is the single beam current. The available cryogenic power must be sufficient to cope with this load which has a contribution that increases with the beam current. The total higher order mode (HOM) power $P_{HOM} \propto I_bI_e$ that could be absorbed by the superconducting cavities was another restriction on the total beam current at LEP. An upgrade of the couplers and RF cables was required to cope with this limitation. Clearly the design of the cavities for the future lepton collider should take advantage of the experience gained while operating LEP.

2.3 Synchrotron radiation power and beam-beam limited regime

Here we specify the design strategy keeping the beam-beam parameter and the synchrotron radiation power constant. The beam-beam parameter depends on the bunch intensity while the power depends on the beam intensity. Hence we will determine the bunch intensity N_b from ξ_y and the number of bunches M_b from P_T while ensuring that the maximum bunch intensity stays below the threshold required to avoid the transverse mode coupled instability.

Writing the emittances in the transverse planes as

$$\epsilon_y = \kappa\epsilon_x$$

where κ is the coupling ratio, the bunch intensity can be expressed as

$$N_b = \left(\frac{2\pi}{r_e} \sqrt{\frac{\kappa \beta_x^*}{\beta_y^*}} \xi_y \right) \gamma \epsilon_x \tag{2.8}$$

where the factors within brackets are assumed to stay constant. One could imagine another scenario with optics changes where $\beta_x^*, \beta_y^*, \kappa$ are allowed to vary.

The equilibrium emittance ϵ_x is determined by the equilibrium between damping and quantum fluctuations and is given approximately by

$$\epsilon_x = \frac{C_q}{J_x} \frac{R}{\rho} \frac{\gamma^2}{\nu_x^3} , \qquad C_q = \frac{55 \hbar c}{32\sqrt{3}(m_e c^2)} = 3.83 \times 10^{-13} [\mathrm{m}] \tag{2.9}$$

Here R is the average radius of the arc assumed to be made of periodic structures such as FODO cells and ν_x is the arc tune. If L_c, μ_c are the length of each periodic cell and the phase advance over the cell respectively, then

$$\nu_x = \frac{2\pi R}{L_c} \frac{\mu_c}{2\pi} = R \frac{\mu_c}{L_c} \tag{2.10}$$

Hence

$$\epsilon_x = \left(\frac{C_q}{J_x} \frac{R}{\rho} [\frac{L_c}{\mu_c}]^3 \right) \frac{\gamma^2}{R^3} \tag{2.11}$$

The factor R/ρ - the ratio of the arc radius to the bend radius - can be treated as constant. Typically it has a value somewhere between 1.0 and 1.25. The arc radius is determined from the machine circumference C in terms of a filling factor f_1. Thus

$$R = f_1 \frac{C}{2\pi} , \quad \text{and} \quad \rho = f_2 R , \qquad f_1, f_2 < 1 \tag{2.12}$$

where f_1, f_2 are held constant. Since we do not make optics changes at different stages, we will treat the factor in brackets in Equation (2.11) as constant. The energy in this relation is of course determined from the energy luminosity relation Equation (2.5). Once the emittance is known, the bunch intensity is calculated from Equation (2.8).

The beam current I and the number of bunches are related as $I = e f_{rev} M_b N_b$, hence the maximum number of bunches is found from the total synchrotron radiation power as

$$M_b^{max} = (\frac{P_T}{2C_\gamma}) \frac{\rho}{f_{rev} N_b E^4} \tag{2.13}$$

The factors in brackets are constant while the other factors change with the machine circumference.

2.4 RF parameters

There are two requirements on the RF voltage parameters. The first requirement on the voltage is that the energy gained due to the RF per turn must equal to the energy lost per turn.

$$eV_{RF} \sin \phi_s = U = C_\gamma \frac{E^4}{\rho} \tag{2.14}$$

where $C_\gamma = (4\pi/3)r_e/(m_e c^2)^3 = 8.86 \times 10^{-5}$m/GeV^3. The second requirement is that the RF acceptance ΔE_{RF} must be a certain number, say N_{QL}, times the rms energy spread σ_E for an acceptable quantum lifetime,

$$\Delta E_{RF} = N_{QL}\sigma_E \tag{2.15}$$

or

$$\sqrt{\frac{1}{\pi h \eta_{slip}} eV_{RF} E G(\phi_s)} = N_{QL}\sqrt{\frac{C_q}{J_s \rho}}\frac{E^2}{m_e c^2} \tag{2.16}$$

where

$$G(\phi_s) = 2\cos\phi_s - (\pi - 2\phi_s)\sin\phi_s \tag{2.17}$$

J_s is the longitudinal damping partition number. Typically we require $N_{QL} \sim 10$. These two conditions can be solved to find the synchronous phase as the solution of the transcendental equation

$$\cot\phi_s + \phi_s - \frac{\pi}{2} - \frac{55\sqrt{3}}{256}\frac{h\eta_{slip}}{J_s \alpha_f}\frac{N_{QL}^2}{\gamma} = 0 \tag{2.18}$$

where $\alpha_f = e^2/(4\pi\epsilon_0 \hbar c) = 1/137.04$ is the fine structure constant. This equation can be solved numerically. Once the synchronous phase is known, the RF voltage can be found from Equation (2.14).

The RF frequency or the harmonic number is related to the desired bunch spacing. In order to accomodate both beams symmetrically around the ring, it is required that the bunch spacing be an even multiple of the RF wavelength. This in turn requires that the harmonic number be an even multiple of the number of bunches. The choice of RF frequency influences the energy acceptance $(\Delta E/E)_{accep}$ because $(\Delta E/E)_{accep} \propto 1/\sqrt{h}$ so lower RF frequencies increase the acceptance. However two economical factors argue for higher frequencies: (1) smaller frequencies increase the size and hence the cost of the cavity and (2) high power klystrons are more cost effective above frequencies of 300MHz. In superconducting cavities the frequency is limited from above by several factors: (1) cavity losses increase with frequency, (2) longitudinal and transverse shunt impedances scale like ω_{RF} and ω_{RF}^2 respectively, (3) the ratio of the energy removed by a bunch from the cavity to the stored energy in the cavity also increases with frequency. In this paper we will consider RF frequencies in the neighbourhood of 400MHz.

As an example, consider a circumference of 228km. We will develop a parameter list based on this circumference. We will assume a total synchrotron radiation power of 100MW and a beam-beam parameter $\xi_y = 0.1$. The maximum number of bunches M_B^{max} determined by Equation (2.13) is 89. The revolution frequency is 1.315kHz and the harmonic closest to 400MHz is 304212 = $2\times(2\times3\times25351)$. This does not have many divisors so a more convenient harmonic number is 304220 = $2\times(2\times5\times7\times41\times53)$. If we accept the requirement that $h = 2nM_B$, the allowed number of bunches less than M_B^{max} are $2, 10, 14, 35, 70, 82$.

2.5 Optics

2.5.1 Arc optics

The choice of phase advance per cell μ_c and the length of a cell L_c are crucial design parameters. The equilibrium emittance decreases as the phase advance increases, reaches a minimum at 135°

and then increases again at larger values of μ_c. The horizontal dispersion also decreases with increasing phase advance and shorter cell lengths. Conversely, stronger focusing also increases the chromaticity and hence the strength of the sextupoles required to correct the chromaticity. Strong sextupoles can limit the available dynamic aperture. For these reasons, the choice of phase advance per cell in electron machines is usually limited in the range of $60^\circ \leq \mu_c < 120^\circ$. For example, LEP started operation with $(60^\circ, 60^\circ)$ phase advances in the (x, y) planes at 45GeV, and since then has used $(90^\circ, 60^\circ)$, $(90^\circ, 90^\circ)$ and $(102^\circ, 90^\circ)$ phase advances at higher energies.

Another parameter affected by the choice of optics is the threshold current for TMCI. From Equation (2.6) we observe that $I_{thresh}^{TMCI} \propto \nu_s/(\sum_i \beta_i k_{\perp\, i})$. To estimate the dependence on μ_c, L_c we replace β_i by the average value in a FODO cell $\langle\beta\rangle = L_c/\sin\mu_c$. The synchrotron tune $\nu_s \propto \sqrt{\alpha_C}$ where α_C is the momentum compaction. Since $\alpha_C \propto 1/\sin^2(\mu_c/2)$, we find

$$I_{thresh}^{TMCI} \propto \frac{\nu_s}{\langle\beta\rangle} \propto \frac{1}{L_c}\cos(\frac{\mu_c}{2}) \tag{2.19}$$

Hence the TMCI threshold is raised with shorter cell lengths and shorter phase advance per cell.

In this paper we will choose the phase advance per cell $\mu_c = 90^\circ$ and then choose a cell length L_c so that the bunch intensity does not exceed a certain threshold set by the TMCI. We will develop parameter sets (luminosity, energy, RF voltages,...) for different machine circumferences in this paper. As we increase the ring circumference μ_c, L_c will be assumed constant while the revolution frequency decreases and the bunch intensity always stays below the TMCI threshold.

The phase advance per cell is one way of controlling the equilibrium emittance. Another way is to redistribute the equilibrium emittance between the horizontal and longitudinal planes by changing the RF frequency. In an lattice constructed entirely of FODO cells, the change of partition number with momentum deviation is given by

$$\frac{dJ_x}{d\delta} = -\frac{dJ_s}{d\delta} = -4\frac{L_D}{L_Q}\left[\frac{2+\frac{1}{2}\sin^2\mu_C/2}{\sin^2\mu_C/2}\right] \tag{2.20}$$

where L_D, L_Q are the lnegth of dipoles in a half cell and length of a quadrupole respectively. Writing $J_x(\delta) = J_x(0) + (dJ_x/d\delta)\delta + \ldots$, we observe that reducing the emittance ϵ_x by half requires increasing the damping partition number to $J_x(\delta) = 2J_x(0)$ or a momentum shift of $\delta_{\Delta J_x=1} = 1/(dJ_x/d\delta)$ if initially $J_x(0) = 1$. The required RF frequency shift is related to the momentum deviation δ by

$$\frac{\Delta f_{RF}}{f_{RF}} = -\frac{\Delta R}{R} = -\alpha_C\delta \tag{2.21}$$

While the horizontal emittance can be changed by an appropriate shift in RF frequency, there is also a change in the radial excursion ΔR of the beam. It is important to keep this as small as possible both to minimize a loss in physical aperture and avoid a significant reduction in the transverse quantum lifetime. A lower phase advance per cell and a shorter quadrupole length relative to the dipole length, i.e. weaker focusing, help to keep the relative change in RF frequency and radial excursion small. As an example we consider the 228km ring whose parameters will be given later in Section 5. With $L_D = 103.7$m, $L_Q = 4.1$m, $\mu_C = 90^\circ$, $\alpha_C = 0.28 \times 10^{-4}$, we find the damping aperture to be $\delta_{\Delta J_x=1} = 2.2 \times 10^{-3}$. The corresponding radial excursion

is about $\Delta R = 1.84$mm. Since this changes the damping partition number by one, we can write this as the change in damping partition per unit of radial excursion,

$$\frac{\Delta J_x}{\Delta R} = 0.54 \ /[\mathrm{mm}]$$

This is large enough to be useful.

An alternative method of reducing the transverse emittances is to place a damping wiggler in a region where the dispersion vanishes. Conversely the emittance could be increased if required, e.g. to reduce the beam-beam tune shift, by placing the wiggler where the dispersion is non-zero.

If the horizontal emittance is reduced by any method, the energy spread increases which decreases the energy resolution of the experiments and also the longitudinal quantum lifetime if the RF voltage is kept constant. This places constraints on the allowed emittance manipulations.

2.5.2 Interaction Region

A detailed design of the IR must include the focusing scheme to obtain the desired spot sizes, a beam separation scheme, the collimation and masking scheme to protect components from synchrotron radiation, local chromaticity correction if required, the interface with the detectors etc. Here we will consider only the basic optics parameters. The lower limit on β^* is usually determined by the maximum tolerable beam size in the interaction region (IR) quadrupoles and the chromaticity generated by these quadrupoles. Furthermore to prevent the loss of luminosity due to the hourglass effect, β^* should be significantly greater than the bunch length.

Here we will assume that $\beta_y^* \ll \beta_x^*$ as is true at most $e^+ - e^-$ rings. Consequently aperture and chromaticity limitations will first arise in the vertical plane. As stated earlier in this section we will consider fixed values of β_x^*, β_y^* at all circumferences and energies and assume that these do not pose aperture restrictions at any energy. These values will need to be reconsidered during the design of the final focusing system.

The choice of β_y^*/β_x^* needs to be closely related to the emittance coupling ratio $\kappa = \epsilon_y/\epsilon_x$. The horizontal beam-beam parameter is related to the vertical parameter as

$$\xi_x = \left[\sqrt{\frac{\kappa}{\beta_y^*/\beta_x^*}}\right] \xi_y \tag{2.22}$$

If $\kappa > \beta_y^*/\beta_x^*$, then $\xi_x > \xi_y$. In this case the beam-beam limit is reached first in the horizontal plane. Beyond this limiting current, the emittance grows linearly with current and the beam-beam parameters stay constant. In particular the vertical beam-beam parameter ξ_y never reaches its maximum value and since the luminosity is proportional to ξ_y, the maximum luminosity is not obtained. It is therefore desirable to have $\kappa \leq \beta_y^*/\beta_x^*$. In this paper we will consider the so called *optimal coupling* scenario where $\kappa = \beta_y^*/\beta_x^*$ and the beam-beam limits are attained simultaneously in both planes, $\xi_x = \xi_y$.

2.6 Operation with many bunches

`to be filled in`

2.7 Polarization

`to be filled in`

2.8 Summary of design strategy

Input parameters

- Maximum synchrotron radiation power.
- Maximum beam-beam parameter.
- Maximum bunch intensity limited by TMCI.
- β_x^*, β_y^*.
- Emittance coupling ratio $\kappa = \epsilon_y/\epsilon_x = \beta_y^*/\beta_x^*$.
- Arc filling factor f_1, ring filling factor f_2.
- Phase advance per cell μ_C.
- Number of IPs.
- N_{QL}: Ratio of RF bucket height (energy acceptance) to rms energy spread.

Output parameters

1. For a given machine circumference C, determine the bend radius ρ and arc radius R from Equation (2.12) with assumed values of f_1, f_2.
2. Determine the maximum energy at this circumference from Equation (2.5).
3. Determine the equilibrium emittance at this energy and maximum bunch intensity from Equation (2.8).
4. Determine the cell length from Equation (2.11).
5. Determine the maximum number of bunches from Equation (2.13).

3 Lifetime

The radiative Bhabha scattering process $e^+e^- \to e^+e^-\gamma$ is expected to dominate the beam lifetime at collision in this large lepton collider. The lifetime from this process with a scattering cross-section $\sigma_{e^+e^-}$ is

$$\tau_L = \frac{1}{N_{IP}} \frac{M_b N_b}{\mathcal{L}\sigma_{e^+e^-}} \tag{3.1}$$

Substituting for the luminosity from Equation (2.4) we can write this in terms of the beam-beam parameter ξ_y as

$$\tau_L = \left[\frac{2r_e}{N_{IP}}\frac{\beta_y^*}{\xi_y}\frac{1}{\sigma_{e^+e^-}}\right]\frac{1}{\gamma f_{rev}} \tag{3.2}$$

The cross-section $\sigma_{e^+e^-}$ has a weak logarithmic dependence on energy (see Equation (A.25) in Apendix A) which can be ignored to first order. Assuming that β_y^*, ξ_y are constant, the terms in square brackets above can be considered nearly constant. At a fixed circumference, the luminosity lifetime decreases with approximately the first power of the energy.

There are other contributions to the beam lifetime such as beam-gas scattering and Compton scattering off thermal photons but those lifetimes are about an order of magnitude larger than the luminosity lifetime considered above. For present purposes those effects can be ignored but need to be considered at a later stage.

4 Scaling of the beam-beam parameter

The damping time τ_s determines the time it takes for the beam to reach an equilibrium distribution in the absence of external nonlinear forces. As the damping increases and this time decreases, the beam becomes more immune to non-resonant perturbations that would change this equilibrium distribution. Indeed observations at several $e^+ - e^-$ colliders have shown that the limiting value of the beam-beam parameter increases slowly with energy or more precisely with the damping decrement. The damping decrement for beam-beam collisions is defined as the inverse of the number of beam-beam collisions per damping period,

$$\lambda_d = \frac{1}{N_{IP}\tau_s} \tag{4.1}$$

where τ_s is the damping time measured in turns. For example at LEP, the beam-beam limit has increased by more than 50% as the energy was increased from 45.6GeV to nearly 100GeV. Fitting a power law to the LEP data [2] for the maximum beam-beam tune shifts at three different energies we find that

$$\xi_{y,max} \sim \lambda_d^{0.26} \tag{4.2}$$

Earlier Keil and Talman [5] and more recently Peggs [6] considered the scaling of the beam-beam tune shift with λ_d applied to data from earlier machines such as SPEAR, PETRA, CESR and found roughly the same power law behaviour.

5 Design Parameters

The design strategy has been outlined in Section 2. We know for example that at fixed luminosity, synchrotron radiation power and beam-beam parameter that the maximum energy of the beams scales with the cube root of the circumference. Here we apply this strategy to different machines with circumferences in the range from 120km to 500km. This should span the range envisoned for different versions of the VLHC.

One feature of the design that needs some iteration is the initial choice of the beam-beam parameter. We have seen in Section 4 that the maximum beam-beam parameter scales with some

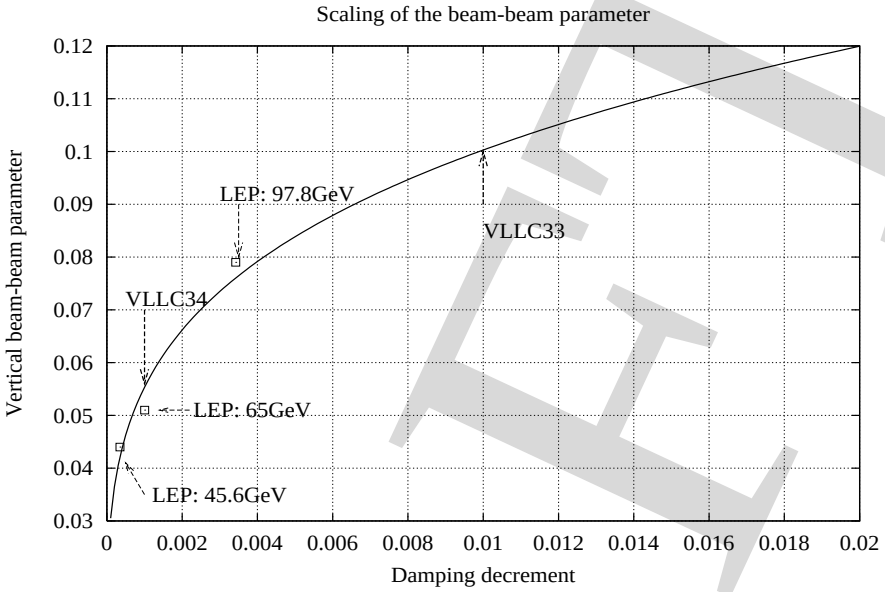

Figure 1: The LEP data on the maximum beam-beam tune shift is fit to a power law curve. Also shown are the damping decrements and expected maximum beam-beam parameter for the VLLC33 (luminosity=10^{33}cm^{-2}sec^{-1}) and VLLC34 (luminosity=10^{34}cm^{-2}sec^{-1}) design parameters.

Figure 1 shows this power law curve and also the expected beam-beam tune shifts for VLLC33 and VLLC34. The damping decrement for VLLC33 is 0.01 which implies $\xi_{y,max} = 0.1$ while for VLLC34 where the maximum energy is lower, $\lambda_d = 0.0006$ and the expected $\xi_{y,max} = 0.05$.

power of the energy. Since the beam energy is an output parameter, we need to ensure that the choice of the beam-beam parameter is self-consistent with the design energy.

Figure 2 shows the maximum energy as a function of the circumference for three different luminosities. For example at a circumference of 228km, the maximum single beam energies at luminosities of $10^{32}, 10^{33}, 10^{34}$ cm^{-2}sec^{-1} are 396, 184 and 70GeV respectively. Thus a ring with circumference around 228km should suffice to reach the top quark production threshold, estimated to be at 360GeV, with a luminosity close to 10^{33}cm^{-2}sec^{-1}. One also observes that single beam energies from 300-500GeV appears attainable at a luminosity of 10^{32}cm^{-2}sec^{-1}. However the RF voltages required in this range of energies is in the hundreds of GV as seen in Figure 3. In the range of 150-250 GeV per beam and luminosity 10^{33}cm^{-2}sec^{-1}, the RF voltages are a few GV, comparable to LEP.

Figure 4 shows the $e^- - e^+$ bremmstrahlung lifetime as a function of circumference at three luminosities. We observe that at a luminosity of 10^{33}cm^{-2}sec^{-1}, this lifetime ranges from 15-36 hours which should be adequate considering that this is the dominant contribution to the beam lifetime at luminosity. The lifetime was calculated using the expression (A.25) for the bremmstrahlung cross-section which does not have corrections from a cut-off parameter which corresponds to the characteristic distance between particles in the bunches. With this cut-off the cross-sections are typically 30% lower. For example analysis of the cross-section at LEP energies [17] showed that the uncorrected cross-section of 0.3barns was reduced to 0.2barns. This number was

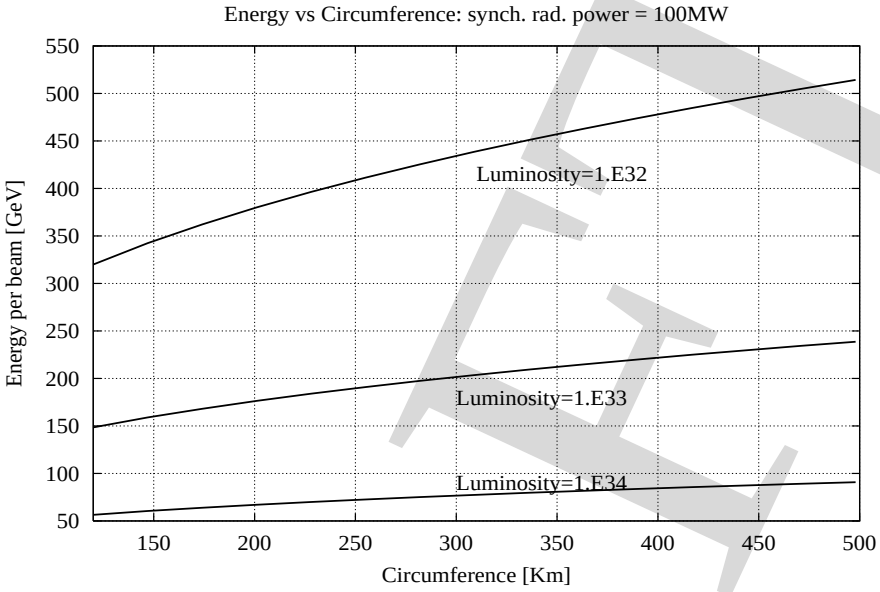

Figure 2: The maximum energy attainable as a function of the machine circumference for three different luminosities. At the energies obtainable with luminosities of 10^{33}cm^{-2}sec^{-1} and lower, the maximum beam-beam parameter was set to 0.1. At the luminosity of 10^{34}cm^{-2}sec^{-1}, the beam-beam parameter was set 0.05. The synchrotron radiation power of both beams was set to 100MW in all cases.

found to agree well with measurements. As a consequence of the smaller cross-section, luminosity lifetimes may be about 30% higher than shown in Figure 4. At most energies, the lifetime is typically in the tens of hours and increases to hundreds of hours when the energy drops to less than 100GeV as is the case when the required luminosity is 10^{34}cm^{-2}sec^{-1}. By comparison, the luminosity lifetime at LEP is about 5-6 hours.

Table 1 shows the design parameters of a 228km ring obtained by following the design strategy outlined in Section 2. We remark on some of the interesting features of this ring compared to LEP.

- Increasing the circumference of LEP by a factor of 8.5 and the total synchrotron radiation power by about 7 allows a 10 fold increase in luminosity at almost double the energy.
- The bunch current in VLLC33 is roughly 5 times lower in keeping with the expected lower threshold for TMCI.
- The $e^+ - e^-$ bremmstrahlung lifetime in VLLC33 is significantly longer at 23 hours.
- The vertical beam sizes in the two machines are comparable
- The horizontal beams sizes in the arcs of the two machines are also close. Hence vacuum chamber dimensions in VLLC33 can be similar to those in LEP.
- The main dipole field is about 5 times weaker than that of LEP. Iron magnets operated at room temperature will suffice. Conversely, good shielding from stray magnetic fields, e.g. those of the low field hadron collider, will be critical.

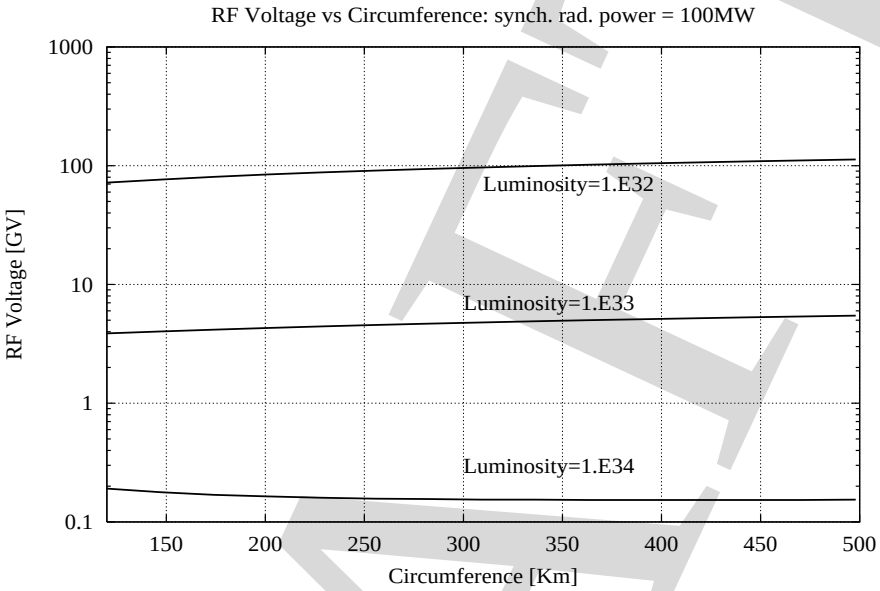

Figure 3: RF voltage required as a function of the machine circumference for different luminosities with the synchrotron radiation power of both beams was set to 100MW in all cases.

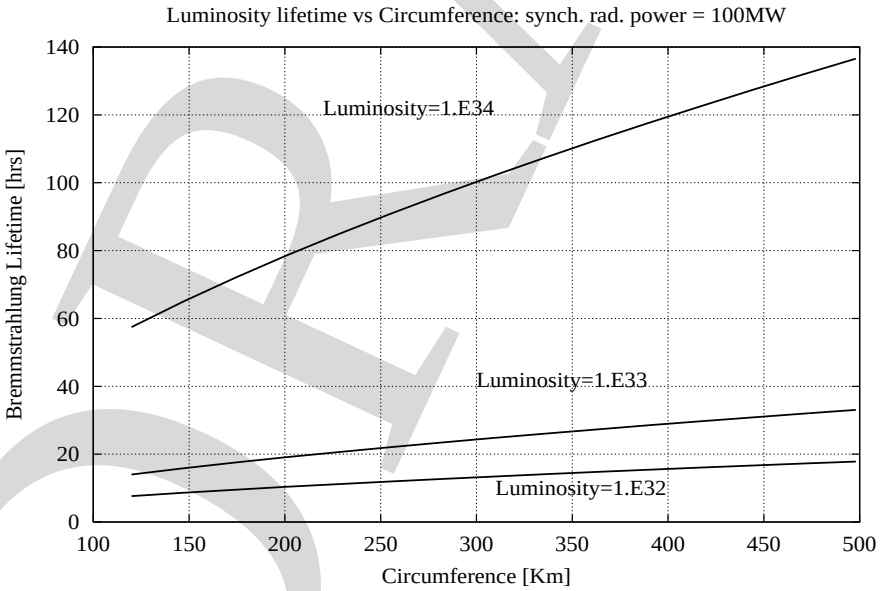

Figure 4: Luminosity lifetime vs the circumference at three different luminosities. Here the lifetime *increases* with the required luminosity because the maximum energy decreases at higher luminosities and the lifetime $\sim 1/E$, cf. Equation(3.2). See the text for other remarks.

$e^+ - e^-$ **Collider Parameters**

Parameter	LEP 1999	VLLC33
Circumference [m]	26658.9	228000
Maximum Energy [GeV]	**97.8**	**184**
Luminosity [cm^{-2}sec^{-1}]	9.73×10^{31}	1×10^{33}
Emittances ϵ_x, ϵ_y [nm]	21.1, 0.22	8.3, 0.415
β_x^*, β_y^* [cm]	150, 5	100, 5
RMS Beam size at IP σ_x^*, σ_y^* [μm]	178, 3.3	91, 4.6
Bunch intensity/current [/mA]	4.01×10^{11}/0.72	6.7×10^{11}/0.14
Number of bunches per beam	4	89
Bunch spacing [km]	6.66	2.56
Total beam current (both beams) [mA]	5.76	25.04
Beam-beam tune shift ξ_x, ξ_y	0.043, 0.079	**0.1**, **0.1**
e^+e^- bremmstrahlung lifetime [hrs]	6	23
Dipole field [T]	0.11	0.024
Bend Radius [m]	3026.42	25411
Phase advance per cell μ_x, μ_y [degrees]	102, 90	90, μ_y
Arc tune	70.3, 62	193, Q_{yC}
Cell Length [m]	79.11	248
Total length of dipoles in a cell [m]	69	207
Quadrupole gradient [T/m]	9.5	28
Length of a quadrupole [m]	1.6	4.1
Arc β^{max}, β^{min} [m]	144, 18	423, 73
Arc $\sigma_x^{max}, \sigma_x^{min}$ [mm]	1.7, 0.6	1.9, 0.8
Arc dispersion D^{max}, D^{min} [m]	1.03, 0.45	1.37, 0.65
Bend radius to Machine radius $2\pi\rho/C$	0.71	0.70
Momentum compaction	1.6×10^{-4}	2.8×10^{-5}
Energy loss per particle per turn [GeV]	2.67	3.99
Critical energy [keV]	686	455
Longitudinal damping time [turns/msec]	73/6.5	46/35
RMS relative energy spread	1.52×10^{-3}	1.0×10^{-3}
Bunch length [mm]	11	7.5
Synchrotron tune	0.116	0.133
RF Voltage [MV]	**3050**	**4660**
RF frequency [MHz]	352.209	400.0
Revolution frequency [kHz]	11.245	1.315
Synchrotron radiation power - both beams [MW]	14.5	100
Available RF power [MW]	34.1	
Power load from both beams [kW/m]	0.82	0.52
Photon flux/length from both beams [/m/sec]	2.4×10^{16}	2.3×10^{16}

Table 1: Parameters of the very large lepton collider with a desired luminosity of 10^{33} cm^{-2}sec^{-1} and a circumference of 228km. For comparison the parameters of LEP during 1999 are also shown (taken from [2]).

- Synchrotron radiation in quadrupoles may be significant. The ratio of the field in a quadrupole at an amplitude equal to the rms beam size to the dipole bend field is a rough measure of this effect [10]. The quadrupole gradient in the VLLC is 28T/m so this ratio is 2.2 which is large. By comparison, in LEP where the gradient is 9.5T/m, this ratio is more than ten times smaller at 0.15. One way to reduce this would be to increase the quadrupole length keeping the same integrated strength. `This needs to be carefully looked at.`

- The critical energy is smaller in VLLC33 so shielding against synchotron radiation as in LEP should be adequate for VLLC33. The photon flux per unit length is almost the same in the two machines.

- The RF voltage required for VLLC33 is significantly higher at 4.7GV (without beam loading) compared to 3.1GV (presumably with beam loading) for LEP.

- We assumed $f_1 = f_2 = 0.84$ to have the same ratio of bend radius ρ to the machine radius $C/(2\pi)$ as in LEP. A somewhat more aggressive choice of packing fractions $f_1 = f_2 = 0.90$ or $2\pi\rho/C = 0.81$ yields slightly different parameters, e.g. maximum energy $E_{max} = 193$GeV, RF voltage $V_{RF} = 4883$MV. Both of these quantities scale with the third root of the bend radius.

- We chose optimum coupling, i.e. $\epsilon_y/\epsilon_x = \beta_y^*/\beta_x^*$ which implies that $\xi_x = \xi_y$. Operating at the beam-beam limit in both planes might well be challenging. If we reduce the emittance coupling to half this value, $\epsilon_y/\epsilon_x = 0.025$, then $\xi_x = 0.071$ while staying at the beam-beam limit in the vertical plane $\xi_y = 0.1$. With this choice, optics and beam size parameters change, e.g. $\epsilon_x = 11.8$nm, cell length=278m, $\beta^{max} = 475$m, $D_x^{max} = 1.72$m, $\sigma_x^{max} = 2.4$mm, $\nu_s = 0.156$, $\sigma_l = 8.1$mm. The RF voltage increases to 4780MV while most other parameters are relatively unaffected.

- We chose an energy acceptance that is ten times the equilibrium energy spread of the beam to ensure sufficient quantum lifetime. At LEP with the parameters given in Table 1, this ratio is only about 6.6. If we assume this value for the 228km ring, the RF voltage is lowered from 4.66GV to 4.43GV. The energy loss per turn requires that the RF voltage be greater than 4GV.

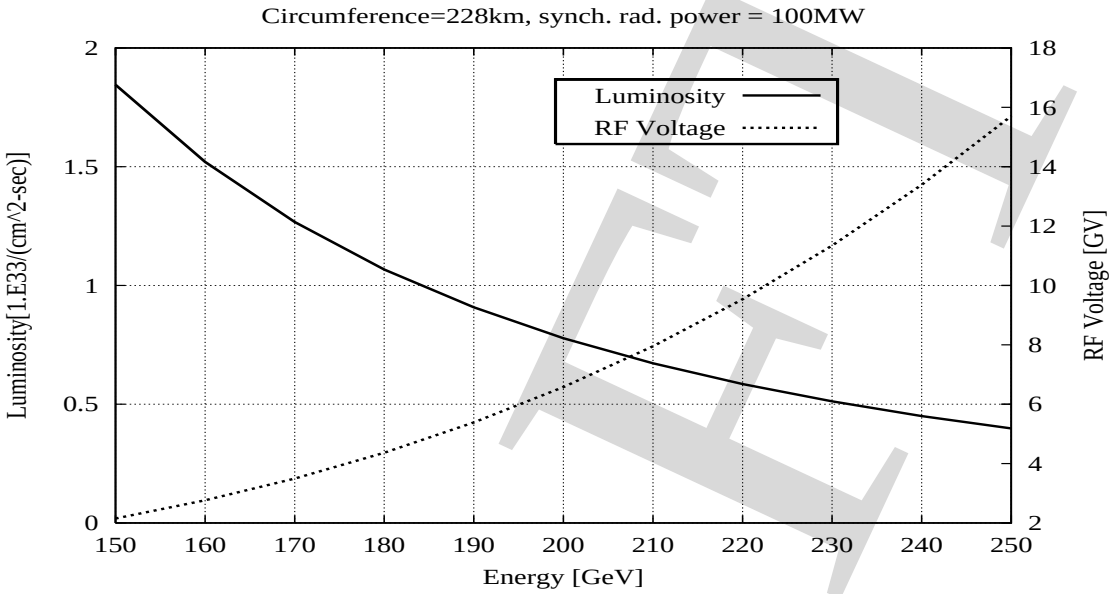

Figure 5: Achievable luminosities and the RF voltages required as a function of energy at a ring circumference of 228km. The synchotron radiation power is kept constant at 100MW.

Once the circumference is chosen, the range of available energies and luminosities is of primary interest. We know that the luminosity falls as E^{-3} and the RF voltage required increases as E^4 when the energy is increased. Figure 5 shows the values of luminosity and RF voltage as a function of energy with a ring circumference of 228km and synchotron radiation power kept constant at 100MW. We observe that if a maximum of 18GV of RF is available, the energy reach of a single beam in this ring extends to 250GeV with luminosities in the range from 0.4-1.8 $\times 10^{33}$cm^{-2}sec^{-1}.

6 Scaling Laws

6.1 Scaling with radius

If the $e^+ - e^-$ collider is to be part of a staged approach to a large tunnel housing both lepton and hadron accelerators which will be ugraded in energy and/or luminosity over time, then it makes sense to consider how the lepton collider parameters scale with the machine radius. This would help determine an optimum radius. Furthermore, once the parameters are determined at one circumference, the scaling laws may be used to calculate the parameters at any other circumference. Table 2 shows the scaling with radius of some of the important parameters.

- Due to the strong dependence of the emittance on the focusing in the arcs, the emittance actually *decreases* with machine radius even though the energy has increased.
- The bunch intensity also decreases with increasing radii and faster than the emittance in order to keep the beam-beam tune shift constant.

Parameter	Radius dependence
Maximum Energy E	$\rho^{1/3}$
Equilibrium emittance $\epsilon_x \sim \gamma^2/R^3$	$\rho^{-7/3}$
Bunch intensity $N_b \sim \xi_y \gamma \epsilon_x$	ρ^{-2}
Maximum number of bunches $M_B^{max} \sim \rho/(f_{rev} N_b \gamma^4)$	$\rho^{8/3}$
RF voltage $V_{RF} \sim \gamma^4/\rho$	$\rho^{1/3} \sim \gamma$
Relative energy spread $\sigma_E/E \sim \gamma/\sqrt{\rho}$	$\rho^{-1/6}$
Synchrotron frequency $\nu_s \sim \sqrt{hV_{RF}\eta/E}$	$\rho^{1/2}$
Bunch length $\sigma_l \sim 1/\omega_s(\sigma_E/E)$	$\rho^{1/3}$
Critical energy $E_c \sim \frac{\gamma^3}{\rho}$	const.
Damping time $\tau_s \sim E^3/\rho$	const.
Maximum beam-beam parameter $\xi \sim \tau_s^{-0.26}$	const.
Bremmstrahlung lifetime $\tau_L \sim 1/(f_{rev}\gamma)$	$\rho^{2/3}$

Table 2: Scaling of beam parameters with machine radius. Luminosity and synchrotron radiation power are kept fixed.

- The number of bunches must be increased to avail of the maximum RF power when the machine radius is increased. There is an upper bound to the number of bunches set for example by the minimum bunch spacing and also from operational considerations.
- The required RF voltage and the maximum energy both increase with the cube root of the machine radius.
- The relative energy spread decreases very slowly as the machine size increases.
- The critical energy does not change as the machine size is increased.
- The damping time measured in turns and therefore the damping decrement λ_d and maximum beam-beam parameter ξ_y also do not change with machine size.

6.2 Scaling with energy

The useful energy reach of the accelerator of fixed circumference can be found by an examination of the scaling of the important parameters with energy. Table 3 shows some of the scaling relations. Most of these dependences on energy are well known. The additional twist here is that the beam-beam parameter is allowed to scale with energy and recent data (see Section 4) suggest that $\xi_y^{max} \sim \gamma^{0.8}$. If we are to operate at the beam-beam limit at all energies, then (a) the luminosity drops more slowly with energy $\mathcal{L} \sim \gamma^{-2.2}$ compared to γ^{-3} without the scaling of the beam-beam parameter and (b) the bunch intensity increases more rapidly as $N_b \sim \gamma^{3.8}$ rather than γ^3. The $e^+ - e^-$ bremmstrahlung lifetime also drops faster with energy as $\tau_L \sim \gamma^{-1.8}$ in this scenario.

Parameter	Energy dependence
Equilibrium emittance ϵ_x	γ^2
Energy loss U_0, RF Voltage V_{RF}	γ^4
Damping time $\tau_s \sim E/U_0$	γ^{-3}
Maximum beam-beam parameter $\xi_y \sim \tau_s^{-0.26}$	$\gamma^{0.8}$
Luminosity $\mathcal{L} \sim \xi_y \gamma^{-3}$	$\gamma^{-2.2}$
Bunch intensity $N_b \sim \xi_y \gamma \epsilon_x$	$\gamma^{3.8}$
Maximum number of bunches $M_B^{max} \sim 1/(N_b E^4)$	$\gamma^{-7.8}$
Synchrotron frequency ν_s	$\gamma^{3/2}$
Equilibrium energy spread σ_E/E	γ
Bunch length σ_l	$\gamma^{-1/2}$
Critical energy E_c	γ^3
Bremmstrahlung lifetime $\tau_L \sim 1/(\xi_y \gamma)$	$\gamma^{-1.8}$

Table 3: Scaling of beam parameters with energy. Machine circumference and synchrotron radiation power are kept fixed.

7 An Injector System

The Fermilab accelerator complex (Linac, Booster and Main Injector) could be used as the basis for an e^+e^- injector if the beam energies were somewhat reduced from those used for protons. The specifications of of an injector system could follow the design of the LEP[11] and HERA[12] injectors, or the the APS[13] injection system.

Two new electron linacs would be required. The first would operate at about 3 GHz and accelerate electrons to an energy of around 200 MeV, which would be sufficient to produce positrons. A positron production target would be followed by a second linac section to produce a positron energy high enough to inject into the positron damping ring. Since the positrons will be produced at a much lower flux and larger emittance than electrons it is necessary to damp and collect positrons from many pulses before further acceleration. The CERN, HERA and APS damping rings are very compact, and operate at energies of around $400 - 600$ MeV. During the checkout of the FNAL 805 MHz linac upgrade, the linac tunnel was operated essentially with two parallel linacs, so the addition of a e^+e^- linac line would not crowd the existing facility[14].

We have considered the use of the FNAL Booster to accelerate the e^+ and e^- to higher energies, however the use of gradient magnets in the lattice makes this ring somewhat inappropriate for electrons since this lattice affects the damping partition numbers in undesirable ways. In order to eliminate this problem, a correction package, consisting of a gradient magnet and a quadrupole, should be inserted in the ring to correct the damping partition numbers. The booster has sufficient space to accommodate this package. Similar packages have been used in the PS at CERN.

It is unclear if it is more efficient to reverse the magnetic field in the accelerator structure or build injection lines so beams could circulate in opposite directions. We assume injection and extraction systems would have to be added to the booster for e^+e^- operation. The maximum energy that could be reached with the existing rf would be around 3 GeV. Since a new proton

source is being considered for a neutrino source and muon collider, which would not fit in the existing booster tunnel, There is also the possibility of designing a compact magnet lattice to replace the existing booster magnets.

We assume electrons and positrons would be injected into the Main Injector, (MI), in opposite directions at an energy of around 3 GeV. This energy would require the MI magnets to operate at a much lower field than would ever be used for protons, however the magnets have been measured at this low field and the field quality seems to be acceptable for electron operation[15]. The maximum energy that could be produced in the main injector is around 12 GeV, due to the limited rf, and the limited space for adding more. The beams would then be extracted in opposite directions into the VLHC booster tunnel for acceleration up to the injection energy of the VLHC ring.

The primary constraint on the injection energy into the e^+e^- collider ring seems to be the remanent fields in the collider magnets at low fields, which could complicate injection. If the 12 GeV electrons from the MI were injected into the collider ring, the average magnetic field would be around 13 Gauss, which should be compared to the 215 Gauss injection field of LEP. It is unclear at this time how low the injection field can be, but it seems likely a desirable injection energy would be in the range of 30-50 GeV. We have studied the properties of an electron ring in the tunnel of a low field VLHC booster in the context of an ep collider[16]. Such a ring could have a maximum energy up to about 80 GeV with a installed RF voltage of 1.09 GV. We assume this rf operates at 352 MHz. If the VLHC booster ring was used only as an injector, an injection energy of around 40 GeV could be accommodated with an rf voltage of about 60 MV.

8 Synchrotron Radiation Source

TO BE FILLED IN

9 Technological Challenges

The primary technical challanges seem to be cooling the vacuum chamber, disposing of the heat produced, and determining how low the field of the collider magnets can be confidently run, since this minimum field determines the design of the magnets and the injection energy. In addition, however, there are a number of other technical problems which must be considered.

- The vacuum chambers and the pumping system must be able to cope with the high levels of synchrotron radiation. Although the power radiated per unit length is less than that at LEP, the small beam size in the arcs mean local power densities can be high. The large bending radius tends to make even energy deposition on the inside of the vacuum chamber difficult. Although lumped and distributed absorption of the synchrotron radiation power are possible we assume that there will be lumped absorbers located near vacuum pumps.

  The hot water produced in the synchrotron absorbers is also a problem. Since there will be roughly 100 MW of heating, distributed over 230 km, we assume this heat must be brought to the surface where cooling towers would be used to discharge it into the atmosphere. This system would be a significant environmental perturbation on the surface. We have also looked at discharging the heat into the ground and into surface water.

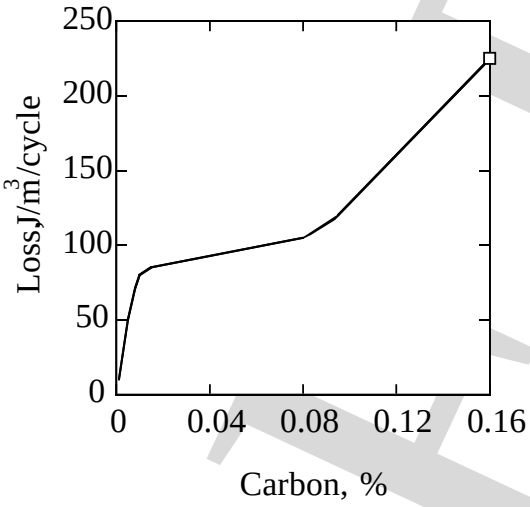

Figure 6: Hysteresis loss as a function of carbon content in steel.

The vacuum chambers themselves are assumed to be bakable, and this introduces a large number of expansion joints into the design. These joints complicate the beam stability, and the requirement for expansion introduces significant mechanical complexity to an otherwise fairly simple vacuum system.

- The primary issue with the injector system design is determining the minimum field where the ring magnets can usefully transport beam. Since the bending magnets in the arcs operate at a field of $B_{inj}[Gauss] = 1.3E[GeV]$, and the error fields at injection should be below $\sim 10^{-3}B_{inj}$, error fields due external sources, other components and remanent fields, could be a problem. A final injector synchrotron must then be designed which can produce beams in the required energy. This synchrotron can be located in the tunnels which would be eventually occupied by the hadron booster.

  We have shown that external fields can be well attenuated by the magnet yoke itself and extensive shielding of magnets may not be required[3] [**?**]. The remanent fields at low excitation are a function of the specific alloy used, and number of alloys exist with very low remanent fields, however their costs tend to to be higher than steel. One option seems to be the use of vacuum or hydrogen annealed steel [**?**]. This anneal removes carbon from the steel very efficiently, reducing the remanent field and hysteresis loses by a significant factor, as shown in the Figure 5, [**?**]. It seems as though an order of magnatude reduction in remanent fields from the standard low carbon 1010 alloy, ($\sim$ 0.1%carbon), may be, in principle, possible, in an alloy which is not significantly more expensive than standard commercially produced ones.

- We assume that superconducting RF cavities will be necessary. The design of these cavities must suppress higher order modes efficiently.

- It is not clear if the $e^+ - e^-$ collider arcs would be optimized with one or two rings. While it is possible to assume that pretzel orbits can produced in the comparatively long arcs, it

is not clear if parisitic collisions will produce significant emittance growth to justify the construction of a second set of arc magnets. This may significantly affect the cost.

- The placement of the rf cavities will determine the energy of the beam around the ring. Since so much energy is added per turn, it may be necessary to distribute the cavities around the ring. This might require zero dispersion straights at a number of locations.

- If the $e^+ - e^-$ collider and the low field hadron collider magnets are both energized at the same time, the lepton collider will need to be protected from the fringe fields of the hadron collider. These fringe fields at a distance of about a meter are of the order of a few hundred Gauss, about the same level as the main bending field in the lepton collider.

- Extensive masking and collimation systems will be required to protect the detector components from synchrotron radiation.

10 Conclusions

We have explored the feasibility of a large electron-positron collider within the context of a staged approach to building a very large hadron collider. We have shown that in a ring of circumference 228km, a lepton collider with $300 \leq E_{cm} \leq 500$GeV with synchrotron radiation power limited to 100MW would require RF voltages from 2-18 GV and would achieve luminosities in the range 0.4-1.8 $\times 10^{33}$cm^{-2}sec^{-1}. The achievable energy extends to nearly 800GeV (center of mass) at a lower luminosity of 10^{32}cm^{-2}sec^{-1} but almost 100GV of RF voltage is required to replenish the energy lost by the beam. We believe that a lepton collider in a tunnel built to house a very large hadon collider is technically feasible. The important question to answer first is whether the physics at these energies is sufficiently interesting. Assuming that is the case, the design of such an accelerator can proceed to the next stage. The cost of the technical components in the lepton collider will likely be dominated by the superconducting RF cavities. Improvements in design and technology can be expected to reduce the cost a decade from now compared to what they are today. Several technical challenges have to be faced but none appear to be insurmountable.

Acknowledgements

We thank Ernie Malamud for initiating this study, ...

References

[1] Annual VLHC meeting, October 2000, Port Jefferson

[2] D. Brandt et al., *Accelerator Physics at LEP*, Reports on Progress in Physics, **63**, 939 (2000)

[3] J. Norem, E. Keil, *A High Energy $e^+ - e^-$ collider in a "Really Large" Tunnel*, ANL-HEP-CP-96-94, 1996

[4] V. Shiltsev, J. Marriner, V. Danilov, *Beam Instabilities in the VLHC*

[5] E. Keil, R. Talman, *Part. Acc.*. , 1983

[6] S. Peggs, Workshop on Synchrotron Radiation Effects in the VLHC, BNL (Sept 2000)

[7] H. Wiedemann, Nucl. Instr. Methods, **172**, 33 (1980)

[8] M. Sands, SLAC Report SLAC-121 (1970)

[9] A. Chao

[10] E. Keil, CERN, personal communication (1999)

[11] The LEP Injector Study Group, *LEP Design Report: Vol.I, The LEP Injector Chain* CERN-LEP/TH/83-29, 1983.

[12] G. Stange, IEEE Trans. Nucl Sci. **NS-26** (1979) 4146.

[13] *Annex to 7-GeV Advanced Photon Source Conceptual Design Report*, Argonne Report ANL-87-15 Annex, (1987).

[14] R. Noble, Fermilab, Private Communication, (1997)

[15] B. Brown, Fermilab, Private Communication, (1997)

[16] M. Derrick, H. Friedsam, A. Gorski, S. Hanuska, J. Jagger, D. Krakauer, J. Norem, E. Rotela, S. Sharma, L. Teng, K. Thompson, T. Sen, E. Chojnacki, D. P. Barber, *An ep Collider with E_{cm}= 1 TeV in a VLHC Tunnel*, Proceedings fo the 1999 Particle Accelerator Conference, New York (1999) 2635

[17] R. Kleiss and H. Burkhardt, Computer Physics Communications, **81**, 372 (1994)

[18] H. Burkhardt, Proceedings of the 3rd Workshop on LEP performance (Chamonix), J. Poole (ed.), CERN SL/93-19

A Appendix: Useful Formulae

Luminosity

$$\mathcal{L} = \frac{N_{e^+} N_{e^-} M_b f_{rev}}{4\pi} \frac{1}{\sqrt{\beta^*_{x,e}\epsilon_{x,e}}\sqrt{\beta^*_{y,e}\epsilon_{y,e}}} \tag{A.1}$$

where N_{e^+}, N_{e^-} are the bunch intensities, M_b is the number of bunches.

Equilibrium horizontal emittance

$$\epsilon_x = \frac{C_q \gamma^2}{J_x} \left[\frac{\oint H/\rho^3 ds}{\oint 1/\rho^2 ds} \right] \tag{A.2}$$

The equilibrium emittance in a lattice built entirely with FODO cells scales with the horizontal phase advance μ_x^C per FODO cell as [7]

$$\epsilon_x(\mu_x^C) = 4\frac{C_q \gamma^2}{J_x}\theta^3 \frac{1 - \frac{3}{4}\sin^2(\mu_x^C/2) + \frac{1}{60}\sin^4(\mu_x^C/2)}{\sin^2(\mu_x^C/2)\sin\mu_x^C}. \tag{A.3}$$

where $C_q = (55/32\sqrt{3})\hbar/mc = 3.84 \times 10^{-13}$m, J_x is the horizontal damping partition number and θ is the bending angle in half of the FODO cell.

Momentum compaction

$$\alpha_C \approx \frac{L_{Arc}}{C} \frac{\theta^2}{\sin^2(\mu_c/2)} \tag{A.4}$$

where L_{Arc}, C are the lengths of the arcs and the circumference respectively, θ is the bend angle per half cell and μ_c is the phase advance per cell.

Equilibrium energy spread

$$\frac{\sigma_E}{E} \simeq \sqrt{\frac{C_q}{J_s \rho}}\,\gamma \tag{A.5}$$

where

$$C_q = \frac{55}{32\sqrt{3}} \frac{\hbar c}{mc^2} = 3.84 \times 10^{-13}\ \mathrm{m}$$

for electrons and positrons. J_s is the longitudinal damping partition number, ρ is the bending radius.

Equilibrium bunch length

$$\sigma_l = \frac{c \mid \eta \mid}{\omega_s} \frac{\sigma_E}{E} = \frac{c}{\sqrt{2\pi} f_{rev}} \sqrt{\frac{\mid \eta \mid E}{heV_{RF}\cos\psi_s}} \frac{\sigma_E}{E} \tag{A.6}$$

where η is the slip factor, ω_s is the angular synchrotron frequency and the other symbols have their usual meanings.

Energy acceptance

$$(\frac{\Delta E}{E})_{accept} = \sqrt{\frac{eV_{RF}}{\pi h|\eta|E} G(\phi_s)} \tag{A.7}$$

$$G(\phi_s) = 2\cos\phi_s - (\pi - 2\phi_s)\sin\phi_s$$

Beam-beam tune shifts

$$\xi_x = \frac{N_e r_e \beta_x^*}{2\pi\gamma\sigma_x^*(\sigma_x^* + \sigma_y^*)} , \qquad \xi_y = \frac{N_e r_e \beta_y^*}{2\pi\gamma\sigma_y^*(\sigma_x^* + \sigma_y^*)} \tag{A.8}$$

In the limit $\sigma_x^* \gg \sigma_y^*$,

$$\xi_x = \frac{N_e r_e \beta_x^*}{2\pi\gamma(\sigma_x^*)^2} , \qquad \xi_y = \frac{N_e r_e \beta_y^*}{2\pi\gamma\sigma_x^*\sigma_y^*} \tag{A.9}$$

Energy lost by electrons per turn

$$U = C_\gamma \frac{E^4}{\rho}, \qquad C_\gamma = \frac{4\pi}{3}\frac{r_e}{(m_e c^2)^3} = 8.86 \times 10^{-5}\mathrm{m/GeV}^3 \tag{A.10}$$

Synchrotron radiation power in beam

$$P_{synch} = \frac{U I_e}{e} \tag{A.11}$$

Critical energy

$$E_{crit}[keV] = 2.218\frac{E^3}{\rho} , \quad E \text{ in GeV} , \rho \text{ in m} \tag{A.12}$$

Critical Wavelength

$$\lambda_{crit} = \frac{4\pi\rho}{3\gamma^3} \times 10^{10} , \quad \text{in Angstroms} \tag{A.13}$$

Number of photons emitted per second by a particle

$$N_\gamma = \frac{15.0\sqrt{3}}{8.0}\frac{P_{synch}}{e N_e E_{crit}} \times 10^3 \tag{A.14}$$

where P_{synch} is in MW, E_{crit} is in keV.

Total Photon Flux

$$\dot{N}_\gamma = 8.08 \times 10^{17} \times I[\mathrm{mA}]E[\mathrm{GeV}], \quad \text{photons/sec} \tag{A.15}$$

Gas Load

$$Q_\gamma = 4.5 \times 10^{-20}\eta_{photo}\phi_\gamma , \qquad [\mathrm{Torr - litres/m/sec}] \tag{A.16}$$

where η_{photo} is the photo-desorption coefficient and $\phi_\gamma = \dot{N}_\gamma / L_{Arc}$ is the photon flux per unit length.

Damping partition numbers

$$J_s \simeq 2.0 \tag{A.17}$$

$$J_x + J_y + J_s = 4 \tag{A.18}$$

For a FODO cell in the thin-lens approximation

$$\frac{dJ_x}{d\delta} = -4\frac{L_D}{L_Q}\left[\frac{2+\frac{1}{2}\sin^2\mu/2}{\sin^2\mu/2}\right] \tag{A.19}$$

Damping times

$$\tau_0 = \frac{E}{f_{rev}U}, \quad \tau_s = \frac{2}{2+\mathcal{D}}\tau_0 \approx \tau_0, \quad \tau_y = 2\tau_0, \quad \tau_x = \frac{2}{1-\mathcal{D}}\tau_0 \approx \tau_y \tag{A.20}$$

$$\mathcal{D} = \frac{\langle\frac{D}{\rho^2}(\frac{1}{\rho}+2\frac{B'}{B})\rangle}{\langle\frac{1}{\rho^2}\rangle} \tag{A.21}$$

Longitudinal quantum lifetime

$$\tau_{quant;s} = \frac{\tau_s}{N_{QL}^2}\exp[\frac{1}{2}N_{QL}^2] \tag{A.22}$$

where

$$N_{QL} = (\frac{\Delta E_{RF}}{\sigma_E})$$

ΔE_{RF} is the energy acceptance of the bucket provided by the RF system, σ_E is the sigma of the energy distribution and τ_s is the longitudinal synchrotron radiation damping time. This is the expression due to Sands [8] but there are other (perhaps more accurate) expressions.

Transverse quantum lifetime

$$\tau_{quant;\beta} = \frac{e^{r_\beta}}{2r_\beta}\tau_\perp \tag{A.23}$$

where

$$r_\beta = \frac{1}{2}(\frac{x_{Apert,\beta}}{\sigma_\beta})^2$$

$x_{Apert,\beta}$ is the transverse position of the aperture limitation, σ_β is the transverse sigma of the particle distribution and $t_{damp,\perp}$ is transverse synchrotron radiation damping time. If there is finite dispersion at the location of the aperture limitation, then Chao's formula [9] holds

$$\tau_{quant;\beta} = \frac{1}{\sqrt{2\pi}}\frac{\exp[r_{\beta,\delta}]}{(2r_{\beta,\delta})^{3/2}}\frac{1}{(1+f)\sqrt{f(1-f)}}\tau_\perp \tag{A.24}$$

where

$$r_{\beta,\delta} = \frac{1}{2}(\frac{x_{Apert,\beta}}{\sigma_T})^2\ , \quad \sigma_T^2 = \sigma_x^2 + D_x^2\sigma_\delta^2\ , \quad f = \frac{D_x^2\sigma_\delta^2}{\sigma_T^2}$$

D_x is the dispersion at the location of the aperture, σ_δ is the relative momentum deviation. For a fixed transverse damping time, the quantum lifetime depends on the parameters $f, r_{\beta,\delta}$ and has minimas at specific values of these parameters.

e^+e^- Bremmstrahlung cross-section

The dominant process which determines the lifetime at collision is small angle forward radiative Bhabha scattering which has a cross-section given by [18]

$$\sigma_{e^+e^-} = \frac{16}{3}\alpha r_e^2 \left[-(\ln(\frac{\Delta E}{E})_{accept} + \frac{5}{8})(\ln(4\gamma_{e^+}\gamma_{e^-}) - \frac{1}{2}) + \frac{1}{2}\ln^2(\frac{\Delta E}{E})_{accept} - \frac{\pi^2}{6} - \frac{3}{8} \right] \quad \text{(A.25)}$$

where $(\Delta E/E)_{accept}$ is the RF acceptance of the bucket.